ACS Catalysis

Research Article

pubs.acs.org/acscatalysis

Phenalenyl in a Different Role: Catalytic Activation through the Nonbonding Molecular Orbital

Sudipta Raha Roy,[†] A. Nijamudheen,[‡] Anand Pariyar,[†] Anup Ghosh,[†] Pavan K. Vardhanapu,[†] Prasun K. Mandal,*[,†] Ayan Datta,*[,‡] and Swadhin K. Mandal*[,†]

[†]Department of Chemical Sciences, Indian Institute of Science Education and Research, 741252 Kolkata, Mohanpur-741246, India

[‡]Department of Spectroscopy, Indian Association for the Cultivation of Science, 2A and 2B Raja S. C. Mullick Road, Jadavpur, 700032 Kolkata, West Bengal, India

Supporting Information

ABSTRACT: We have demonstrated that the nonbonding molecular orbital (NBMO) of the phenalenyl (PLY) cation can be used as a Lewis acid catalyst for different organic transformations. Detailed computational and spectroscopic studies for the aminolysis reaction of epoxide reveal that this catalysis works through a different mechanism, and the phenalenyl cation activates the amine moiety using its empty NBMO, which triggers the epoxide ring-opening reaction. It has been shown that the energy of the NBMO of PLY cation plays a key role in modulating the catalytic activity. This study establishes that the cationic state of phenalenyl unit is useful not only for construction of the spin memory device by external spin injection using its NBMO, but in addition, the same NBMO can act as an organic Lewis acceptor unit to influence the catalytic outcome of a homogeneous reaction.

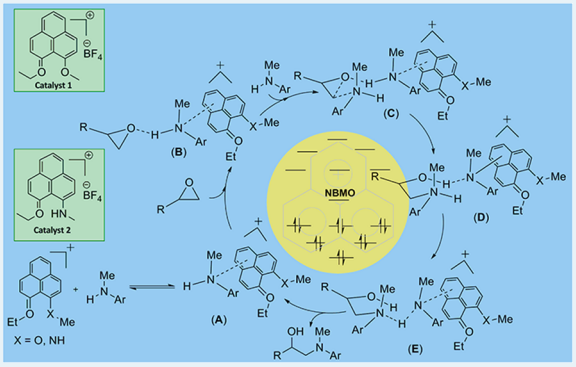

KEYWORDS: *catalysis, organocatalysis, organic Lewis acid, phenalenyl (PLY) cation, nonbonding molecular orbital (NBMO), electrophilic activation, noncovalent interaction*

INTRODUCTION

The phenalenyl (PLY) unit has played an intriguing role in different fields of research spanning from chemistry, to material chemistry, to device physics, acting as a key electronic reservoir. Phenalenyl is a well-known odd alternant hydrocarbon with high symmetry (D_{3h}) which has the ability to form three redox species: cation, neutral radical, and anion.[1] Formation of this redox triad involves the use of the formally nonbonding molecular orbital (NBMO) of the phenalenyl molecule and hence does not greatly affect the stability of the resulting species.[2,3] The transformation from cation to radical to anion of phenalenyl unit progresses through successive electron acceptance in an accessible NBMO as predicted from an early Hückel molecular orbital (HMO) calculations in 1960s.[2] Later, the concept of using this NBMO of phenalenyl was proposed for designing neutral free radical based molecular conductors by Haddon.[3] Subsequently, this idea led to the discovery of the best neutral organic conductor at room temperature.[4] The radical state of phenalenyl molecules has been used as a building block to prepare intriguing materials for exploring new conjugated electronic systems, such as multifunctional electronic and magnetic materials exhibiting simultaneous bistability in multiple physical channels.[4a,5] Until recently, most studies focused on the radical state of phenalenyl based molecules, and recent articles by Morita, Takui, and Hicks describe the present status of phenalenyl based radical materials.[6]

For some time, we started working on another possible electronic state of phenalenyl moiety, where it stays in its cationic state possessing an empty NBMO. Recently, we have demonstrated that the cationic state can be generated by metal ion coordination, and organometallic phenalenyl complexes can act as catalysts, in which the phenalenyl unit played a significant role in modulating the catalytic outcome.[7] Furthermore, we recently demonstrated the potential of cationic phenalenyl moiety in molecular spintronics.[8] A zinc ion coordinated cationic phenalenyl unit in an organometallic compound acted as a spin trap, leading to the development of the phenalenyl based spin memory device.[8] When the nonmagnetic phenalenylorganozinc compound is deposited over a ferromagnetic substrate, the cationic phenalenyl accepts electron from the substrate and becomes magnetic, resulting in an unexpectedly large magnetoresistance of 20% at near room temperature which can be manipulated by external stimuli.[8] This result could provide a platform for developing molecular memory devices of next generation with superior strength,

Received: July 24, 2014
Revised: October 7, 2014
Published: October 22, 2014

   dx.doi.org/10.1021/cs5010695 | ACS Catal. 2014, 4, 4307−4319

which is based on the phenalenyl's ability to accept an electron utilizing its empty NBMO.

In the present study, we used metal-free cationic phenalenyl compounds to design an organic Lewis acid catalyst which utilizes the empty NBMO of phenalenyl for electron acceptance. In this regard, we posed a question whether the presence of this readily available NBMO in the phenalenyl system in its cationic state can be utilized to design well-defined molecular catalysts. It was postulated that the vacant NBMO of phenalenyl unit may have a great influence in catalytic reactions. The initial interaction of the electron density of the approaching nucleophile could be supported by the presence of an energetically accessible orbital of the ligand system (Chart 1). It is now well documented that dramatic enhancement of

Chart 1. (a) Cationic Phenalenyl Compounds 1 and 2; (b) Schematic Description of Molecular Orbitals of Cationic PLY[1a]

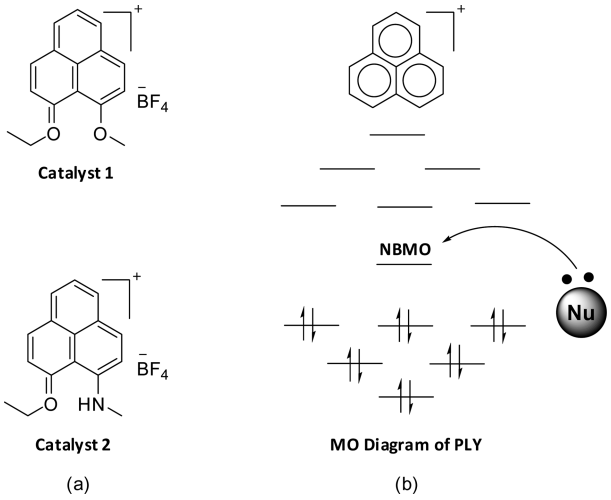

[a]The schema above show that NBMO of PLY cation can support interaction with nucleophilic substrate (Nu).

the catalytic activity can be achieved by modulating the Lewis acidity of the catalyst.[9] In fact, the utilization of a Lewis acid is considered as one of the most versatile ways to facilitate catalysis. By definition, a Lewis acid has a low-lying LUMO that is capable of accepting an electron pair.[10] The majority of Lewis acids are based on metal ions or elements that are electronically unsatisfied and have easily accessible orbitals (for example, boron- and aluminum-based Lewis acids).[9] Moreover, a Lewis acid derived from purely organic molecules is difficult to realize as the LUMO of most neutral organic molecules is antibonding in nature, which is difficult to access energetically during catalysis. Very few conjugated electron greedy molecules have been reported in catalysis.[11]

In this approach, we design organic Lewis acid catalysts using the vacant NBMO of PLY cation which might have specific advantage due to two reasons: the accessibility of the accepting orbital and the use of NBMO will not necessitate compromization on the stability of the transition state unlike in a case when the molecule utilizes a formally antibonding orbital as a major pathway toward the transition state. In the present study, we have chosen a model reaction, namely, the epoxide ring-opening reaction involving amine in the presence of organic phenalenyl cations as catalysts. To the best of our knowledge, not a single organocatalyst system is reported in which the NBMO has been used as the major pathway of interaction, until the contribution of our study.

RESULTS AND DISCUSSION

The phenalenyl (PLY)-based cations (Chart 1a) 9-methoxy-1-ethoxyphenalenium tetrafluoroborate (**1**, O,O-system) and 9-methylamino-1-ethoxyphenalenium tetrafluoroborate (**2**, N,O-system) were synthesized following the reported procedure.[12] For the present study, we have chosen the epoxide ring-opening reaction with amine as a model organic reaction. The epoxide ring-opening reaction is an important one as it can lead to the formation of β-hydroxy amine, which has been key intermediate for the synthesis of several drugs, pharmaceuticals, and natural products.[13] The classical approach for the synthesis of β-hydroxy amine involves Lewis acid based[14] (preferably a metal salt) activation of epoxides followed by nucleophilic attack with amines. As a result, various Lewis acid catalysts[15,16] have been developed for activating the epoxides. As proof of concept, we began the study by testing the catalytic activity of **1** (2.5 mol %) for the model reaction of 2-(phenoxymethyl)-oxirane (**3a**) with *N*-methylaniline (**4a**) under neat condition at 40 °C. To our expectation, the desired β-hydroxy amine, 1-(methyl(phenyl)amino)-3-phenoxypropan-2-ol (**5**) was obtained in 84% yield (Table 1, entry 1). Subsequently, the

Table 1. Standardization of Reaction Condition for the Epoxide Ring Opening[a]

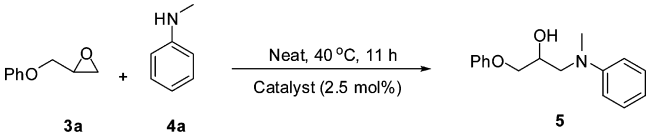

3a 4a 5

entry	catalyst	mol (%)	conversion (%)[b]
1	Catalyst **1**	2.5	84
2	Catalyst **1**	1.25	75
3	Catalyst **1**	5.0	85
4	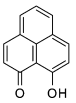	2.5	11
5	$NaBF_4$	2.5	19
6	Blank	---	08

[a]**3a** (2 mmol) was treated with **4a** (2 mmol, 1 equiv) in the presence of catalyst **1** (2.5 mol %) at 40 °C under neat condition for 11 h unless otherwise specified. [b]Conversion was determined by ^{1}H NMR spectroscopy.

amount of catalyst loading was varied to determine the most effective catalytic condition. The use of lesser amount of catalyst **1** (1.25 mol %) has a slight detrimental effect on the overall conversion of the reaction (Table 1, entry 2). The use of greater amounts (5 mol %) of **1** did not provide any beneficial effect in terms of reduction of the reaction time or conversion (Table 1, entry 3). It may be argued that the reaction of the PLY-based catalyst with amine may generate the HBF_4[12a] and the in situ generated acid can catalyze the reaction. When we mixed the catalyst **1** and amine **4a** (in 1:1 ratio, see the following text for further details) and recorded the ^{1}H NMR

dx.doi.org/10.1021/cs5010695 | ACS Catal. 2014, 4, 4307−4319

Table 2. Aminolysis Reaction of Epoxide in the Presence of Catalysts 1 and 2[a]

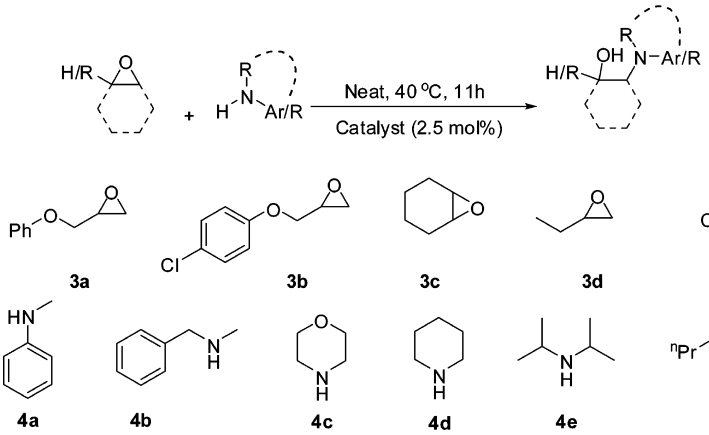

entry	amine	epoxide	yield (%)[b,c]	
			catalyst **1**	catalyst **2**
1	**4a**	**3a**	84 (80)	46
2	**4a**	**3b**	85	72
3	**4a**	**3c**	99 (91)	76
4	**4a**	**3d**	85	60
5	**4a**	**3e**	85 (70)	63
6	**4b**	**3a**	99 (93)	80
7	**4b**	**3b**	99 (95)	86
8	**4b**	**3d**	83 (75)	65
9	**4c**	**3a**	99	72
10	**4c**	**3b**	83	76
11	**4c**	**3d**	98 (90)	82
12	**4d**	**3a**	98 (85)	85
13	**4d**	**3b**	96 (90)	75
14	**4d**	**3d**	94 (80)	73
15	**4e**	**3a**	55	40
16	**4f**	**3a**	93 (75)	74
17	**4f**	**3b**	92 (80)	78
18	**4f**	**3d**	98 (89)	73

[a]The epoxide (2 mmol) was treated with amine (2 mmol) in the presence of catalyst **1** or **2** (2.5 mol %) at 40 °C. [b]Conversion was determined by ^{1}H NMR spectroscopy. [c]Parentheses represent the isolated yield.

spectrum, we did not observe any significant change in chemical shift from either of these two individual moieties, which ruled out the possibility of HBF_4 catalyzed reaction. The parent 9-hydroxyphenalenone, when used as a catalyst, resulted in poor conversion (11%, Table 1, entry 4). In another control experiment, we used $NaBF_4$ as catalyst which also led to very poor catalytic activity (19%, Table 1, entry 5) revealing that the presence of the PLY-based cationic moiety as catalyst has prominent effect on the catalysis. In another control experiment, when this reaction was performed in the absence of catalyst **1**, only 8% (Table 1, entry 6) conversion was observed. This observation confirms the indispensable role of the PLY-based cation during catalysis.

In order to check the versatility of this catalytic process, we investigated the scope of catalyst **1** (2.5 mol %) for the aminolysis reaction of several functionalized epoxides. We also used another PLY-based cation, 9-methyiamino-1-ethoxy-phenalenium tetrafluoroborate (**2**, N,O-system), as catalyst to check the change in efficacy of the catalyst depending on the nature of PLY cation used. Under the optimized procedure, reactions proceed smoothly and gave the corresponding *β*-hydroxy amine in good to excellent yield. The regioselective nucleophilic attack by different amines took place almost exclusively on the less-hindered side of the terminal epoxide (Table 2, entries 1−2, 4−5, etc.). When the cyclohexene oxide (**3c**) was treated with **4a** (Table 2, entries 3), it gave the diastereoselective *trans*-*β*-hydroxy amine exclusively. The reaction of epichlorohydrin **3e** (Table 2, entry 5) provided excellent example of chemo and regioselectivity and afforded 85% yield of the *β*-hydroxy amine corresponding to nucleophilic attack at the terminal carbon of the epoxide moiety. Different electronically and sterically diverse amines were reacted in the presence of catalysts **1** and **2** at 40 °C under solvent-free condition. The reaction rate appeared to be influenced by the nature of the amine (Table 2, entries 1 and 6) as evident from the reaction performed with **4a** (an aromatic amine), resulting in less conversion than with an aliphatic amine **4b**. Treatment of terminal epoxides **3a** and **3b** with morpholine **4c** (Table 2, entries 9−11) and piperidine **4d** (Table 2, entries 12−14) as a congener of cyclic aliphatic amine, gives the corresponding *β*-hydroxy amine in good to excellent yield. A sterically hindered amine, such as di-isopropylamine **4e** (Table 2, entry 15), also works under the optimized condition. We tried to synthesize the *β*-hydroxy amine with long chain acyclic amine. The regioselective nucleophilic attack took place almost exclusively on the less

dx.doi.org/10.1021/cs5010695 | ACS Catal. 2014, 4, 4307−4319

hindered side of the terminal epoxide (Table 2, entry 16−18) upon the treatment of dibutylamine (**4f**) with the terminal epoxides (**4a, 4b**, and **4d**). This methodology is equally effective for aromatic as well as aliphatic amines. The catalytic results reveal that irrespective of amines, reaction proceeds with excellent conversion in case of catalyst **1**. Though there are only very few reports for the epoxide ring-opening reaction in the presence of metal-free catalysts,[16a,c] the present catalysts show comparable or better catalytic activity than the reported metal-free catalysts. Moreover, this catalyst system can stay live for a number of consecutive catalytic cycles without losing the catalytic activity significantly (see Supporting Information for details). As a general observation, it was noticed from Table 2, in all the reactions tested in the present study, the catalyst **1** outperforms catalyst **2** in terms of activity under the identical reaction condition.

We have performed a comparative kinetic study to understand the relative efficacy of catalysts **1** and **2** for the model reaction involving **3a** and **4a** via ^{1}H NMR spectroscopy over the course of the first 6 h (Figure 1). From the kinetic analysis, it is evident that catalyst **1** is superior than that of catalyst **2**, as also observed consistently from the data presented in Table 2.

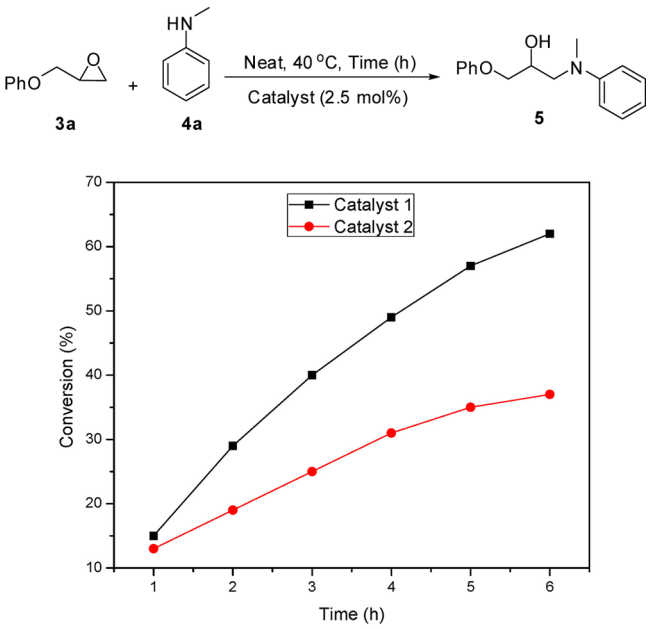

Figure 1. Kinetic studies revealing that catalyst **1** has better efficacy than catalyst **2**.

The difference in reactivity between the catalysts **1** and **2** intrigues us to find its relationship in the molecular level, and therefore, we have carried out density functional theory (DFT) study at the M06-2X/6-31+G(d) level of theory. An analysis of the charge density distributions is shown in Figure 2a. The calculated orbital energy diagrams of **1** and **2** show that the LUMO (see Figure 2b) of these catalysts are largely nonbonding in nature and is highly separated from the LUMO−1 and LUMO+1(Figure 2c). The presence of the NBMO of PLY cation as the LUMO has earlier been predicted for the cationic state of parent phenalenyl molecule.[1,3] The LUMO of catalyst **1** (Figure 2c) is well separated from its nearest molecular orbitals with a calculated LUMO−(LUMO +1) gap of 2.52 eV and a LUMO−1 − LUMO gap of 5.37 eV. At the same time, catalyst **2** has a comparatively smaller LUMO − LUMO+1 gap of 2.34 eV and LUMO−1 − LUMO gap of 5.22 eV. Thus, the DFT calculation supports the presence of energetically accessible empty molecular orbital for electron acceptance in these PLY-based catalysts. Interestingly, the calculation reveals that the relative energy of the LUMO largely depends on the nature of the substitutions in the PLY. In other words, the LUMO energy levels in these PLY units can be tuned by changing the substitution from O,O (in catalyst **1**) to N,O (in catalyst **2**) in the present study (Figure 2c).

To understand the electron-acceptance property of this organic Lewis acid and to further support our DFT-calculation-based findings, we carried out a cyclic voltammetric study. These experiments indeed revealed the presence of two one-electron acceptance processes in both catalyst **1** and **2** (Figure 3a and b, respectively). The $E_{1/2}$ values of **1** ($E^1_{1/2}$ = −0.408 V and $E^2_{1/2}$ = −1.486 V) and **2** ($E^1_{1/2}$ = −0.931 V and $E^2_{1/2}$ = −1.820 V) indicate that electron acceptance from the first to the second one becomes progressively difficult as a result of increasing Coulombic repulsion in the system. A similar observation was also noted by Haddon and co-workers with the 9-ethoxy-1-ethoxyphenalenium tetrafluoroborate system.[17]

Earlier EPR studies on spirobiphenalenyl boron salts[4,18] had shown that the first reduction leads to the formation of an EPR active radical species and the second reduction results in the EPR silent anionic species, supporting our result that the LUMO of a PLY system can accommodate two electrons. The cyclic voltammetry thus in the present case can be explained by considering the generation of a neutral radical and an anionic species (Figure 3c). Comparing first reduction potential data of **1** and **2** [**1** ($E^1_{1/2}$ = −0.408 V) and **2** ($E^1_{1/2}$ = −0.931 V)], it is clear that the reduction of **1** is much more facile than **2**. This result points out that the LUMO of **1** is more accessible for electron acceptance as compared to that of **2**, which is in consonance with our DFT calculation (Figure 2c).

Next, we attempted to envisage the molecular level interaction of the catalyst with the substrates to understand the mechanistic insight of the epoxide ring opening with amine. A general perception for the Lewis acid catalyzed aminolysis reaction of epoxide ring-opening reaction is that a Lewis acid (preferably a metal salt) can activate the epoxide substrate by forming a strong coordinate bond with the oxygen atom of the epoxide ring. This type of interaction increases the electrophilicity of the carbon atoms of the epoxide ring which assists in the opening of epoxide ring.[14−16] However, when catalyst **1** was mixed with amine **4a** in a ratio of 1:1, there was a sharp visual change in color from orange to dark brown. On the other hand, no such sharp color change was observed when we physically mix catalyst **1** and epoxide **3a**. This observation clearly highlights that NBMO-based organic Lewis acid works in a different pathway than the traditional Lewis acid catalyzed aminolysis reaction of epoxide and further prompted us to record a detailed absorption and emission spectra of these mixtures.

We followed the interaction between amine/epoxide (see Supporting Information for epoxide) with the catalyst spectroscopically. After a careful stepwise addition of amine **4a** to a solution of **1** (25 μM), the absorbance of **1** was found to be gradually decreased with increasing the concentration of **4a**. Presence of an isosbestic point (Figure 4a) at 468 nm for **4a** proves beyond any doubt that a ground state interaction has indeed happened with catalyst **1** and **4a**.

dx.doi.org/10.1021/cs5010695 | ACS Catal. 2014, 4, 4307−4319

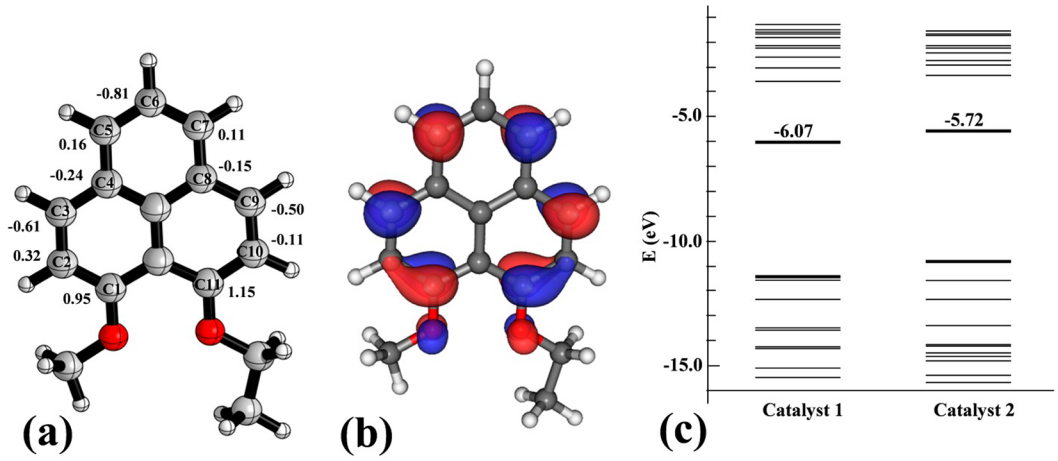

Figure 2. (a) Mulliken charge densities on selected carbon atoms in catalyst **1**. (b) Computed LUMO of the catalyst **1**. (c) Molecular orbital energy profile diagrams of catalysts **1** and **2**. Energy of LUMO level (in eV) is shown.

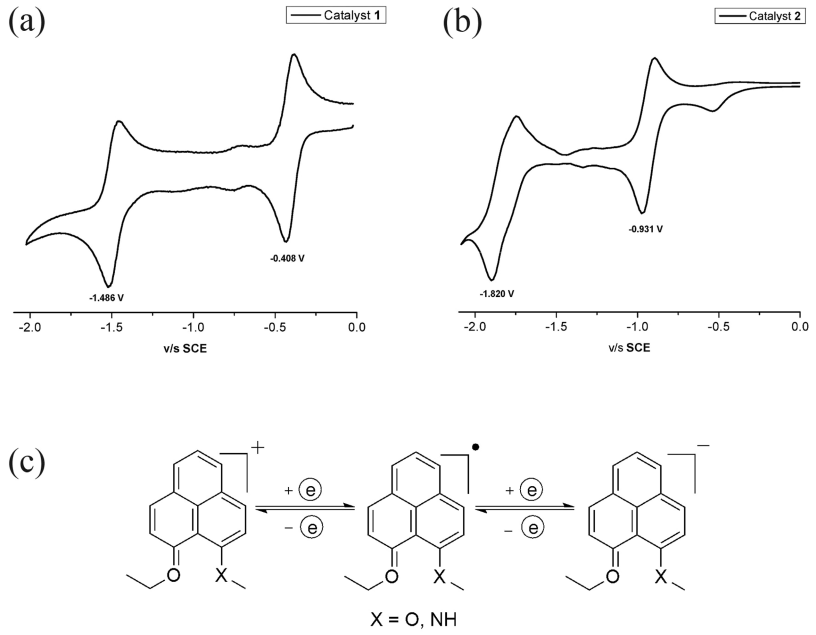

Figure 3. (a,b) Cyclic voltammogram of catalysts **1** and **2** in acetonitrile, referenced to SCE via internal ferrocene revealing two successive one-electron reduction processes. (c) Successive electron acceptance by catalysts **1** and **2** generates a neutral radical and an anionic species.

In order to obtain the stoichoimetry of the amine−catalyst adduct we have carried out Job's plot (ΔOD vs mole fraction of **4a**; where ΔOD = $I_0 - I$; I_0 = absorbance of **1** in absence of **4a**, and I = absorbance of **1** in the presence of quencher **4a**) which clearly demonstrates a 1:1 association of **1** and **4a** (Figure 4b). Further, we have monitored the emission spectroscopy of **1** at different concentration of amine to understand the exact interaction of **1** with **4a**. Sequential addition of **4a** to a solution of **1** (25 μM) resulted in a gradual decrease in the fluorescence intensity of the catalyst **1** (Figure 4c), further confirms the interaction between amine and catalyst. The extent of the interaction has been followed by the Stern−Volmer plot (plot of F_0/F against the concentration of **4a**; where F_0 = fluorescence intensity in absence of any quencher, F = fluorescence intensity in the presence of quencher) (Figure 4d) as well as by Benesi−Hildebrand plot (plot of $1/[F - F_0]$ versus $1/[\mathbf{4a}]$) (Figure 4e). As it can be seen from Figure 4d, a strict linear behavior of the quenching (obtained from Stern−Volmer plot) confirms that the quenching is static in nature.[19a]

We have also estimated the association constant of this process between the **1** and **4a** from emission spectroscopic measurements by using Benesi−Hildebrand equation. From the Benesi−Hildebrand plot (Figure 4e), the cumulative association constant has been calculated to be 13.3×10^3 LM^{-1} for the catalyst−amine pair and that for the catalyst−epoxy pair is 4.8×10^3 LM^{-1} (see Supporting Information for details). These values suggest that the association between catalyst and amine is 2−3 times much stronger than that between catalyst epoxide. Furthermore, to understand the nature of association between catalyst and amine, we mixed the catalyst **1** and amine **4a** (in 1:1 ratio) and recorded the ^{1}H NMR spectrum. We did not observe any significant change in the chemical shift from either of these two individual starting moieties (see Supporting Information for NMR spectra). This NMR experiment clearly suggests that there is no strong association (covalent bond formation) between catalyst **1** and amine **4a**. However, from the absorption and emission spectroscopic studies, we can

dx.doi.org/10.1021/cs5010695 | ACS Catal. 2014, 4, 4307−4319

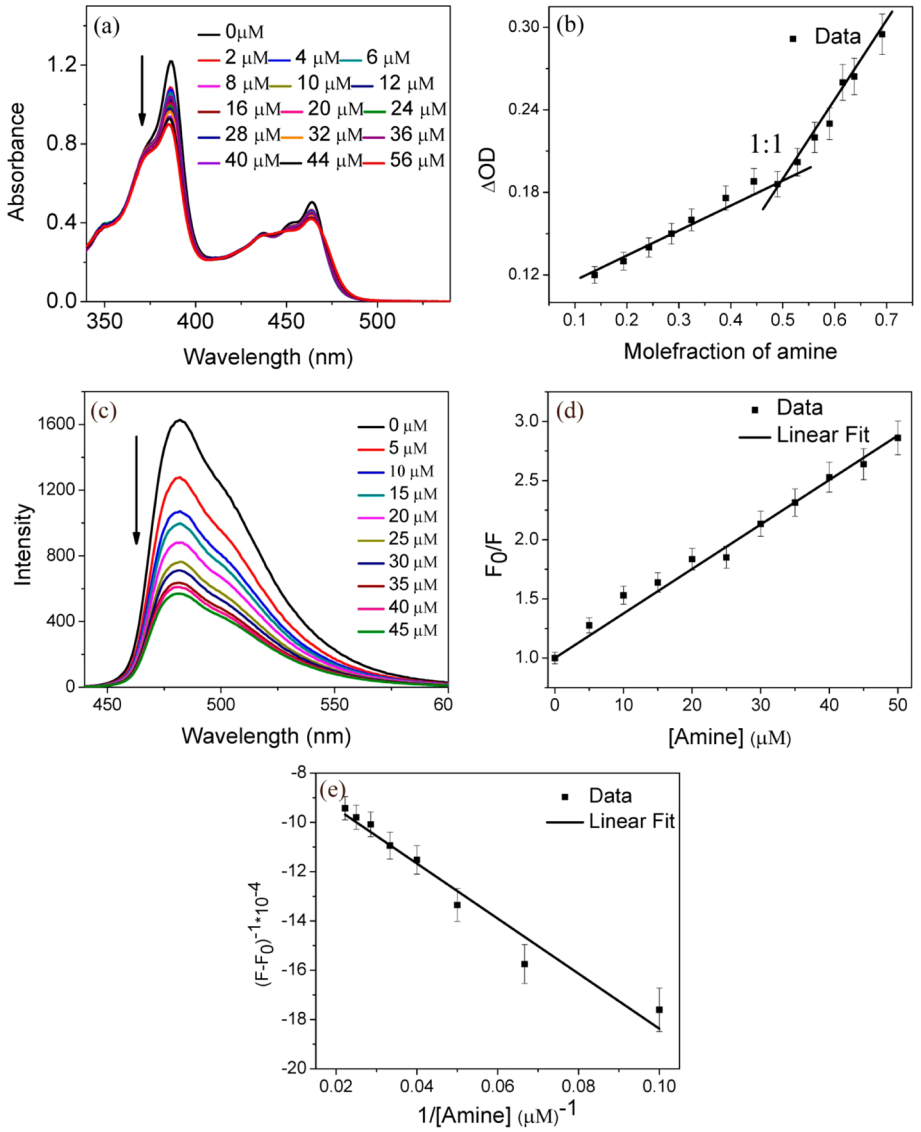

Figure 4. Spectroscopic signature of the binding of catalyst **1** with amine **4a**. (a) Absorption spectra in MeCN. (b) Job's Plot (plot of ΔOD vs mole fraction of amine **4a**). (c) Steady state emission spectra in MeCN. (d) Stern-Volmer plot (plot of F_0/F vs **4a** concentration). (e) Benesi Hildebrand plot (plot of $1/[F - F_0]$ vs $1/[\mathbf{4a}]$). For details see text.

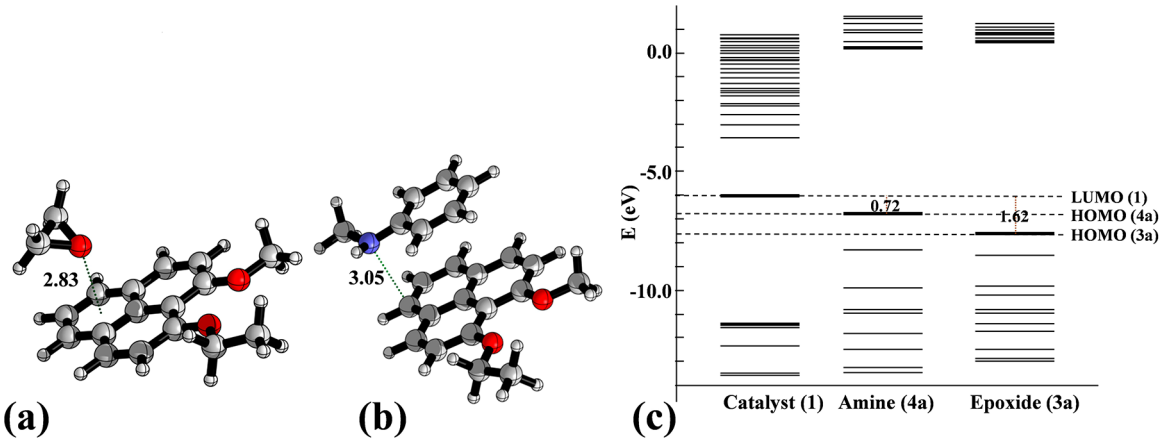

Figure 5. Optimized geometries of catalyst **1** with (a) a model epoxide **3a** and (b) amine **4a**. Selected bond distances (in Å) are shown. (c) Molecular orbital energy profile diagrams of catalyst **1**, amine **4a**, and epoxide **3a**. Energy gaps between the LUMO level of catalyst **1** and HOMO levels of reactants (in eV) are shown.

dx.doi.org/10.1021/cs5010695 | ACS Catal. 2014, 4, 4307−4319

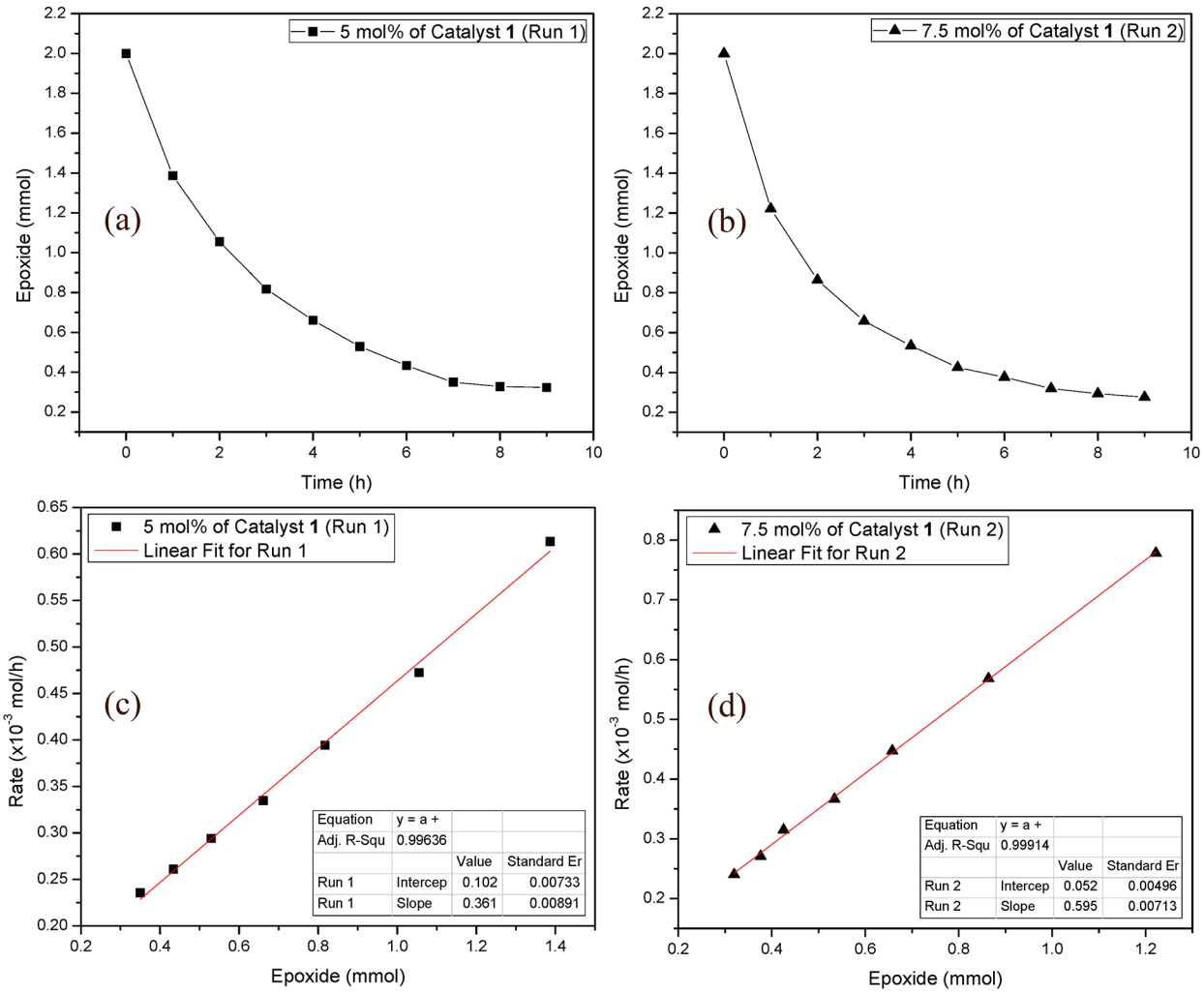

Figure 6. Kinetic studies of epoxide ring-opening reaction for the formation of **5** monitored by ^{1}HNMR spectroscopy in $CDCl_3$. (a,b) Plots showing the change of epoxide concentration with time for the reaction of **3a** (2 mmol), **4a** (2 mol) with varying catalyst **1** concentration. (c,d) Plots of rate (mmol/h) versus epoxide concentration (mmol).

conclude that there is a loose association (noncovalent) between catalyst **1** and amine **4a**.

The spectroscopic results were rationalized on the basis of computations on the interaction of catalyst **1** with both the amine and epoxide reactants. Ethylene oxide was used as the simplified model to mimic the epoxide reactants. Calculations show that epoxide could form a complex with the planar surface of catalyst **1** through the lone pair−π interaction resulting from an interaction of 1:1 mixture of **1** and ethylene oxide as shown in Figure 5a. The distance of 2.83 Å between the aromatic surface of catalyst **1** and epoxide oxygen is within the range of conventional lone pair−π interactions.[19b,c] However, the binding energy of this complex was found to be small. Binding energies obtained for adduct of **1** with epoxide was of ΔE (BSSE corrected) = −5.5 kcal/mol. Also, the Gibb's free energy changes were found to be clearly positive; +2.5 kcal/mol. This suggests a poor association of **1** with epoxide and possibly eliminates the well-documented electrophilic activation of epoxide in the present case.[15,16]

Alternatively, it may be considered that amine might form a more stable adduct with **1** as the nucleophilicity of the nitrogen of the amine is more than that of the oxygen atom of the epoxide. Interactions of catalyst **1** with the amine reactants were then computed using *N*-methylaniline as the model amine (Figure 5b). It is important to note that catalyst **1** can bind with *N*-methylaniline through a large number of stacked and nonstacked orientations in addition to a lone pair−π interaction model. We have optimized all important geometries that could be formed from the binding of **4a** with different binding sites on catalyst **1** to identify the most stable complex (details of the optimized structures and their energetics are tabulated in the Supporting Information). Among them, the most suitable reactive intermediate (Figure 5b) is stabilized by a binding energy of ΔE (BSSE corrected) = −11.1 kcal/mol due to favorable π−π stacking interactions.

Furthermore, it was observed from the calculations that the LUMO of catalyst **1** remains 0.72 eV above the HOMO of amine **4a** while for the HOMO of epoxide **3a**, the LUMO of **1** is placed 1.62 eV above (Figure 5c). Thus, the comparatively shorter HOMO−LUMO gap in the case of adduct formed between **1** and **4a** results in stronger donor−acceptor interaction and initiate the nucleophilic activation. These computational studies are also in agreement with our spectroscopic results.

Detailed kinetic studies were performed following the literature method reported earlier[20] to gain further insight

dx.doi.org/10.1021/cs5010695 | ACS Catal. 2014, 4, 4307−4319

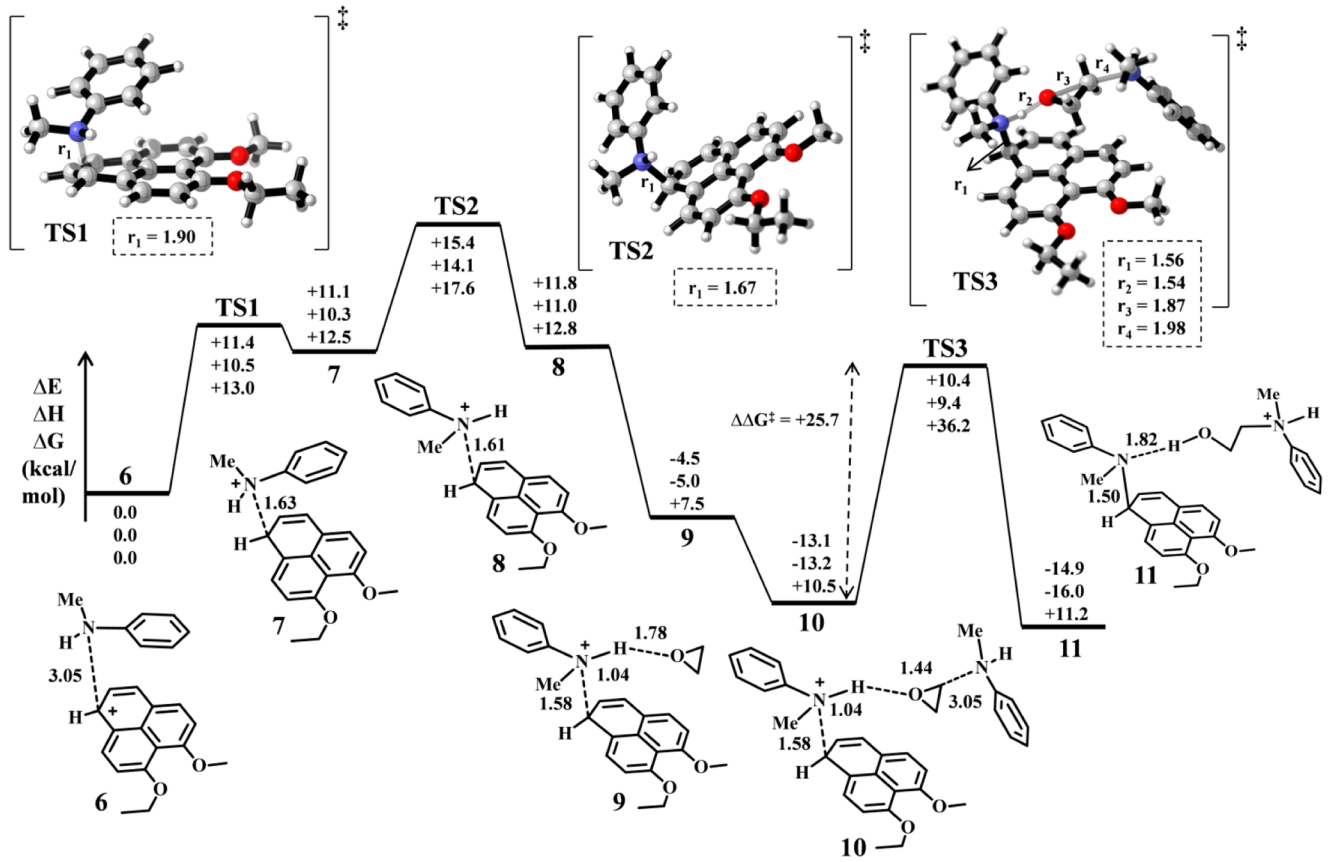

Figure 7. Computed potential energy surface (PES) for the reaction between **4a** and ethylene oxide in the presence of catalyst **1**. Selected bond distances (in Å) and relative energies with respect to the reactants (in kcal/mol) are shown.

into the aminolysis process for the model reaction between **3a** and **4a** under neat condition using **1** as catalyst. Kinetic studies of all the reactions were performed by following the standard optimized reaction condition. The evolution of the specific resonances of the product β-hydroxy amine **5** was monitored by ^{1}H NMR spectroscopy relative to the concentration of either starting amine or epoxide. From this conversion, the effective concentration (mmol) of the **4a**/**3a** over the courses of the first 9 h was determined, which in turn was used for the calculation of rate (mmol/h) of the reaction.

To determine the order of the reaction with respect to catalyst concentration, the aminolysis reaction was carried out in two different concentrations of catalyst **1** (Run 1: with 5 mol % catalyst loading and Run 2: with 7.5 mol% catalyst loading separately) and keeping the concentration of epoxide **3a** (2 mmol) and amine **4a** (2 mmol) fixed. The progress of the reaction was monitored during the first 9 h (Figure 6a,b) which shows gradual decrease of epoxide concentration with time. The amine and epoxide concentration at a given time can be quantified with the help of ^{1}H NMR spectroscopy, and the rate of the reaction can be calculated by determining the conversion at a given time. A plot of rate (mmol/h) versus different epoxide concentrations was determined for two sets of reactions (using two different catalyst concentration), which reveals a linear increase of the reaction rate with epoxide concentration (Figure 6c,d). Comparing the rate of reaction for two sets of catalyst concentration, one can calculate (see Supporting Information for detail) and confirm the first-order dependency of the reaction rate with respect to the catalyst concentration.

Efforts were also given to determine the order of the reaction with respect to the amine concentration as well as with respect to epoxide concentration, respectively, in a similar way (see Supporting Information for details). It shows a second-order dependency of the reaction rate with respect to the amine concentration and a first-order dependency with epoxide concentration.

Thus, from the present study, the overall rate law for the aminolysis reaction of **3a** with **4a** catalyzed by **1** can be summarized as shown in eq 1.

$$\text{Rate} = k[\text{Catalyst}]^1 \times [\text{Amine}]^2 \times [\text{Epoxide}]^1 \ldots\ldots\ldots \quad (1)$$

Subsequently, in order to understand the complete mechanistic cycle and the role of catalyst, we have modeled the reaction between ethylene oxide and **4a** in the presence (or absence) of catalysts **1** or **2**. Calculations at M06-2X/6-31+G(d) level of theory predicted that, in the absence of any catalyst, a very high activation energy ($\Delta\Delta G^{\ddagger}$ = 35.5 kcal/mol) is required for this chemical transformation (see Supporting Information for detail).

The computed potential energy surface for this reaction in the presence of catalyst **1** is shown in Figure 7. The $\pi-\pi$ stacked reactive intermediate **6** can readily undergo two intramolecular rearrangements, first to **7** with strengthening of catalyst−nitrogen bond and then to an unfolded conformation in **8**. Small activation barriers of $\Delta G^{\ddagger}$ = 13.0 kcal/mol (**TS1**) and 5.1 kcal/mol (**TS2**) were found for these rearrangements. Both of these rearrangements occur with strengthening of newly formed C−N bond between the catalyst and reactant as well as with the activation of N−H bond. The

dx.doi.org/10.1021/cs5010695 | ACS Catal. 2014, 4, 4307−4319

Scheme 1. Schematic Presentation of Plausible Mechanism for the Phenalenyl Cation Catalyzed Reaction between Amine with Epoxide Forming β-Hydroxy Amine[a]

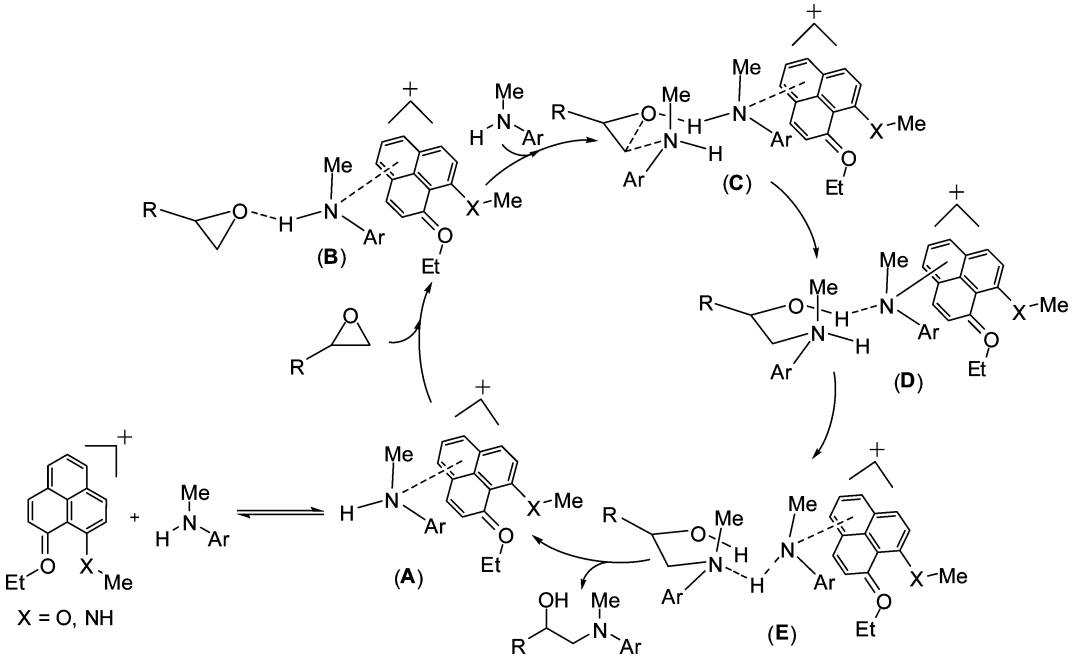

[a]A generalized presentation has been adopted for the sake of simplicity where **A**, **B**, **C**, and **D** represent **6**, **9**, **10**, and **11** of Figure 7, respectively.

C−N bond distance decreases from 3.05 Å in **6** to 1.63 Å in **7** and subsequently shortens to 1.61 Å in the nonstacked, unfolded conformer **8**. At the same time, the N−H bond weakens from 1.01 Å in free **4a** to 1.03 Å in **8**. In addition, the DFT calculations show that the formation of **7** and **8** with shorter C··· N bond distances (1.61−1.63 Å) are endothermic processes, and the reverse reaction to return to the noncovalent adduct **6** should be a rapid processes. This suggests that the amine catalyst adduct stays in a dynamic equilibrium between **6**, **7**, and **8** with low energy barrier. Both the calculations and spectroscopic experiments show that the stable catalyst···amine complex is noncovalent in nature.

In the following step, the epoxide molecule forms a N−H··· O hydrogen bond by interacting with **8** resulting in the intermediate **9**. A second molecule of amine (**4a**) would further activate the reaction by binding with the epoxide carbon atom to form the weakly bound complex **10**. In the succeeding step, the proton abstraction by the epoxide and the formation of a carbon−nitrogen bond between the epoxide and second molecule of amine (**4a**) occurs through the concerted transition state **TS3** to form the complex **11**. In the presence of epoxide, the catalyst amine interaction switches form loose association to a stronger association, and in **11**, the C−N bond distance approaches to 1.5 Å, indicating a covalent type bonding interaction as shown in Figure 7. **11** can undergo a proton transfer process forming the desired product and regenerating **6**.[21] Similar to the uncatalyzed reaction, this step was identified as the rate-determining step. Importantly, the activation energy of 25.7 kcal/mol ($\Delta\Delta G^{\ddagger}$) required to cross the barrier **TS3**, which is significantly lower compared to that of 35.5 kcal/mol required for the uncatalyzed reaction (see Supporting Information for detail).

Thus, our calculations justify the role of catalyst in the reaction profile. Further, our computational results have been corroborated by the experimental kinetic studies, which show that the reaction is second order with respect to the amine and first order with respect to the epoxide and the catalyst (see eq 1).

From the rate law of the reaction between **3a** and **4a** in the presence of catalyst **1**, it suggests the involvement of two molecules of amine with one molecule of each of catalyst and epoxide during the rate-determining step of the aminolysis reaction. This is also reflected in the DFT calculated reaction profile which revealed that the rate-determining step involves one epoxide molecule, two amine molecules, and one catalyst molecule (during the transformation of **10** to **11**, Figure 7). Combining all these results, we propose a schematic presentation of plausible mechanism for the phenalenyl cation based organic Lewis acid catalyzed reaction of amine with epoxide (Scheme 1).

The greater nucleophilicity of the nitrogen atom of the amine moiety in comparison to the oxygen atom of the epoxide prefers stronger interaction between the catalyst and amine-generating catalytically active species **A**. The primary interaction between amine and catalyst in **A** turned out to be a noncovalent type. This is evident from spectroscopic studies and the DFT calculation which have shown that the minimum energy geometry of the initial complex between **1** and **4a** (**6** in Figure 7) is purely noncovalent in nature,[22] and it can be ascertained that there is a loose association between catalyst **1** and amine **4a**. Interestingly, this 1:1 amine−catalyst association in turn activates the hydrogen atom of N−H functionality of the amine and prompts the formation of hydrogen bond with oxygen of the epoxide molecule forming **B**. This hydrogen bonding with epoxide in **B** activates the epoxide molecule by increasing its electrophilicy. Then, the second molecule of amine approaches **B** and forms the intermediate **C** by binding with the epoxide carbon atom at the sterically and electronically favorable site. Subsequently the C−O bond of epoxide breaks, and the new C−N bond between epoxide and second amine

dx.doi.org/10.1021/cs5010695 | ACS Catal. 2014, 4, 4307−4319

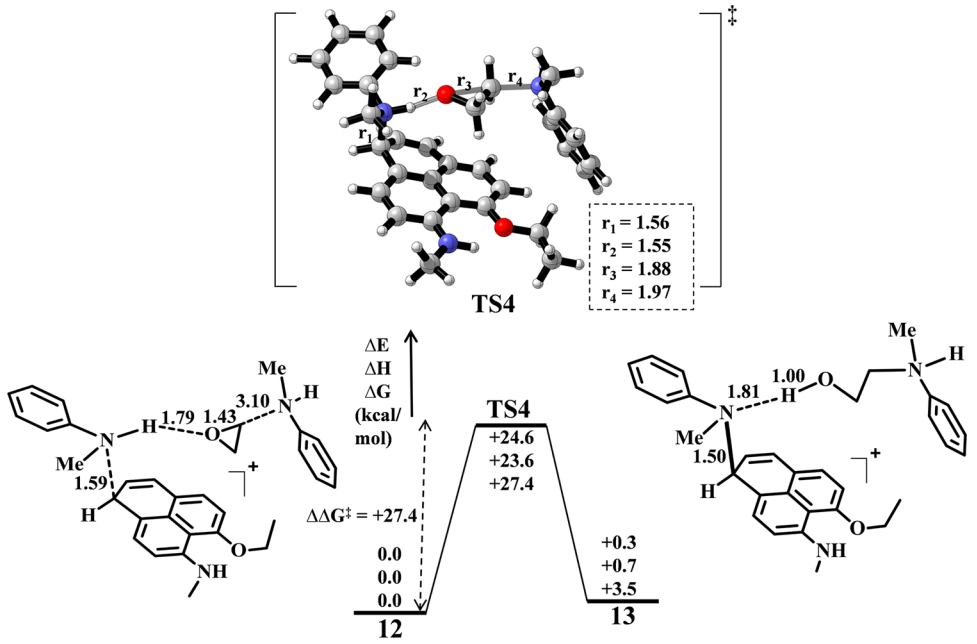

Figure 8. Reaction coordinate for the rate-determining step for the reaction between *N*-methylaniline and ethylene oxide in the presence of catalyst **2**. Selected bond distances (in Å) and relative energies in kcal/mol are shown.

molecule is formed in intermediate **D**. Finally, a proton transfer from **D** via **E** regenerates the catalytically active species **A**. DFT calculation reveals that the Gibb's free energy change is thermodynamically feasible (−23.9 kcal/mol, see Supporting Information for details) for the proton transfer process transforming **D** to **A** forming desired *β*-hydroxy amine via epoxide ring opening and regenerating the catalyst−amine adduct **A**.

Furthermore, to understand the superior activity of catalyst **1** over catalyst **2**, it was found by DFT calculation that the free energy of activation required for the rate-determining step (shown in Figure 8) in the presence of catalyst **2** is higher in energy than the respective barrier **TS3** in the presence of catalyst **1** by 1.7 kcal/mol.

Thus, although catalyst **2** shows significant catalytic activity compared to the uncatalyzed reaction, it is less efficient than the catalyst **1**. Hence, our computational study fully substantiates the experimental findings. The enhanced activity of catalyst **1** could be explained from a comparison of HOMO energy of *N*-methylaniline with LUMO energies of both Lewis acid catalysts **1** and **2**. The LUMO of catalyst **1** lays 0.72 eV above the HOMO of *N*-methylaniline, whereas for catalyst **2**, it is placed 1.07 eV above the HOMO of *N*-methylamine, resulting in a larger HOMO−LUMO gap for catalyst **2** as compared to catalyst **1**. Such significant changes in the catalytic activity were understood on the basis of the fact that the substitution on PLY system can tune its LUMO energy. In general, the substitution of an electron-withdrawing group stabilizes the LUMO, whereas the substitution of an electron-donating group can lead to the reverse effect.

To establish that our concept of using the NBMO of the PLY cation is not limited to only epoxide ring-opening reaction and that the same concept can be extended and generalized for more organic transformations, we tried to check the efficacy of catalysts **1** and **2** in different organic transformations. We can anticipate that NBMO of the PLY cation can also be able to activate the aldehyde. Keeping this goal in mind, we were attracted to utilize these cationic PLY molecules as versatile organic Lewis acids for different aldehyde based reactions, and we planned to use them as catalysts for the synthesis of bis(indolyl)methanes (see Supporting Information for plausible mechanism). The development of new methodologies[23] for the synthesis of bis(indolyl)methanes is a subject of continuous interest to synthetic organic/medicinal chemists as indole and their derivatives have versatile biological activities[24] and are widely present in various biologically active natural products.[25] To examine the effect of the cationic PLY-based molecule, the reaction of indole with 4-methoxybenzaldehyde (Scheme 2) under neat conditions and at room temperature was considered for a model study. An initial screening was done to obtain maximum conversion to the product in short period. The

Scheme 2. Synthesis of Bisindolylmethanes in the Presence of PLY Cations (1 and 2) as Organic Lewis Acid Catalysts

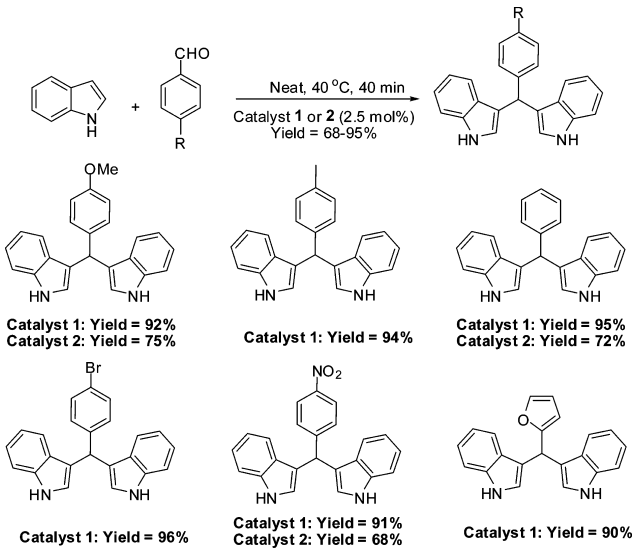

dx.doi.org/10.1021/cs5010695 | ACS Catal. 2014, 4, 4307−4319

progress of the reactions was monitored by TLC taking into consideration the complete consumption of indole. The reaction was completed in 40 min using catalyst **1**. In a control experiment when the model reaction was performed in the absence of catalyst, only 10% desired product was formed. This observation clearly highlights the role of NBMO based catalyst for this chemical transformation.

To establish the generality of the organic Lewis acid catalyzed bisindolylmethane formation, various functionalized aldehydes were treated with indole (Scheme 2). The reaction is compatible with a variety of functional groups as well as with heterocyclic aldehyde. In all cases, the reaction proceeded smoothly at room temperature to afford the corresponding bisindolylmethanes in excellent yields (85−95%). To compare the catalytic activity between the catalysts **1** and **2**, few parallel experiments were performed. Here we also found that catalyst **1** is more effective than catalyst **2**.

Furthermore, we extend this concept of using NBMO based organic Lewis acid concept in multicomponent reactions (MCRs) as well. In recent years, several new criteria have been brought forward in the synthetic process to solve the challenging synthetic problem. Among them, MCRs[26] have been recognized as a new synthetic support. The perpetual interest of synthetic chemists toward the development of newer methodologies for the synthesis of naphthylbenzamide[27] moiety relies on its broad range of biological activities.[28] To confirm the efficiency of the organic Lewis acid catalysts **1** and **2** for MCR transformation, we used a model reaction that comprises a three-component reaction (3-MCR) involving an benzaldehyde, β-napthol, and benzamide in the presence of catalyst **1** (2.5 mol %) at 100 °C under neat condition (Scheme 3). To our delight, the desired naphthylbenzamide was formed in 95% yield after 1 h. However, in the absence of catalyst, very poor conversion was observed.

Encouraged with this preliminary result, we applied this present methodology with the various functionalized aldehydes. Irrespective of functionality, the final product was formed in excellent yield (Scheme 3).

Scheme 3. Synthesis of Naphthylbenzamide in the Presence of PLY-Based Organic Lewis Acid Catalysts 1 and 2

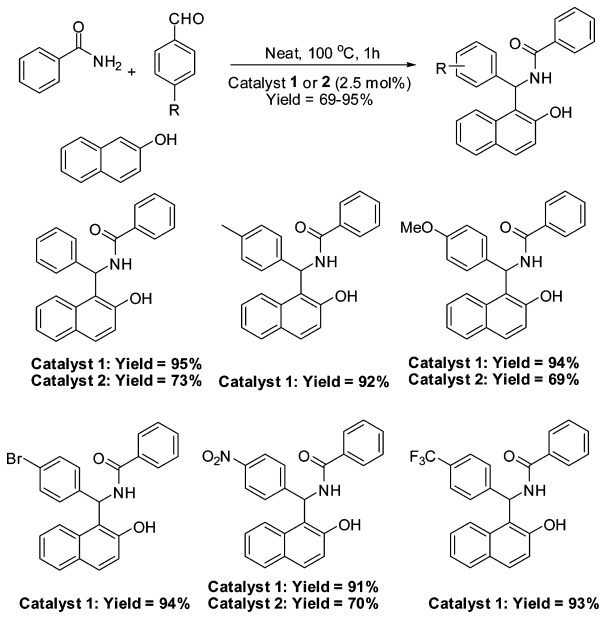

In these MCR reactions, we also observed the consistent catalytic activity ordering between **1** and **2** when the reactions were carried out under identical condition, which shows catalyst **1** is more active in comparison to catalyst **2**.

CONCLUSIONS

In summary, we have demonstrated that the NBMOs of the phenalenyl cation can be used as highly active Lewis acid catalysts for organic transformations such as the epoxide ring-opening reaction with amine in the present case. The chemistry of phenalenyl system started more than six decades back, and a number of phenalenyl-based neutral free radicals have already been realized in the solid state; their promise as fascinating materials has been very well documented. However, with this study, we show that the empty NBMO of organic phenalenyl cation can be utilized as Lewis acid catalyst. This work represents a major step in phenalenyl chemistry, dealing with cationic phenalenyl states to design molecular catalysts using its easily accessible electron-acceptance capability into the empty NBMO. This particular concept was also further successfully extended in different types of organic transformations, showing the versatility of cataionic PLY as organic Lewis acid. Furthermore, we have shown that by chemically tuning the energy of NBMO of PLY cation, one can alter the Lewis acidity, and eventually, it can change the catalytic outcome of the reaction. This phenomenon clearly describes the importance of the NBMO mediated organocatalysis.

EXPERIMENTAL SECTION

General Considerations. All solvents were distilled from Na/benzophenone prior to use. All chemicals were purchased from Aldrich and Fluka Chemicals and used as received. The ^{1}H and ^{13}C NMR spectra were recorded on 400 and 500 MHz spectrometer in $CD_3CN/CDCl_3/DMSO$-d_6 with residual undeuterated solvent (CD_3CN: 1.94/1.3, 118.2, $CDCl_3$: 7.26/77.0, DMSO-d_6: 2.5/39.5) as an internal standard. Chemical shifts (δ) are given in ppm and J values are given in Hz. The HR-MS data were obtained using a Q-TOF Micromass. Open-column chromatography and thin-layer chromatography (TLC) were performed on Silica gel [60−120 mesh]. Evaporation of solvents was performed at reduced pressure using a rotary evaporator.

Experimental Procedure for the Cyclic Voltammetry. Cyclic Voltammetry was performed using a PAR potentiostat at room temperature in dry acetonitrile under argon atmosphere with n-Bu_4NClO_4 (0.1 M) as supporting electrolyte. Potentials were scanned with respect to the quasi-reference electrode in a single compartment cell fitted with Pt electrodes (working, auxiliary and reference) and referenced to the Fc/Fc+ couple of ferrocene at 0.38 V versus SCE. The Epa-Epc separation of the reversible couples was within 10% of that of the Fc/Fc+ couple.

Typical Procedure for the Formation of β-Hydroxy Amines (Table 2, Entry 1). A mixture of 2-(phenoxymethyl)-oxirane **3a** (0.30g, 2 mmol) and *N*-methylaniline **4a** (0.214g, 2 mmol, 1 equiv) were stirred magnetically at 40 °C in the presence of catalyst **1** (18 mg, 2.5 mol %). After 11 h, the reaction mixture was diluted with EtOAc (5 mL) followed by addition of water (2 mL). The supernatant EtOAc solution was decanted. The aqueous layer/portion was extracted with EtOAc (2 × 5 mL). The combined EtOAc extracts were dried (Na_2SO_4) and concentrated under vacuum. The conversion of the reaction was checked by ^{1}H NMR spectroscopy. When the

dx.doi.org/10.1021/cs5010695 | ACS Catal. 2014, 4, 4307−4319

crude product was estimated to be greater than 80% pure, flash chromatography (1:0 to 7:3 hexane/EtOAc) was then performed to get the isolated yield of the corresponding pure β-hydroxy amines.

Procedure for the Synthesis of Bisindolylmethane (Scheme 2). A mixture of aldehyde (2 mmol, 1 equiv) and indole (0.464 g, 4 mmol, 2 equiv) was stirred at 40 °C in the presence of catalyst **1** (18 mg, 2.5 mol %) for 40 min. After completion of the reaction (TLC), the mixture was diluted with water (2 mL) and EtOAc (5 mL). The supernatant EtOAc solution was decanted off. The aqueous layer/portion was extracted with EtOAc (2 × 5 mL). The combined EtOAc extracts were dried over Na_2SO_4. The organic phase was concentrated in vacuo, and the purity of the residue was checked by ^{1}H NMR spectroscopy. Flash chromatography was performed with eluant EtOAc/petroleum ether (1:9) unless crude product was estimated to be greater than 95% pure.

Procedure for the Synthesis of Naphthylbenzamide (Scheme 3). A mixture of aldehyde (1 mmol, 1 equiv), 2-napthol (0.144 g, 1 mmol, 1 equiv), and benzamide (0.121 g, 1 mmol, 1 equiv) was stirred at 100 °C in the presence of catalyst **1** (9 mg, 2.5 mol %) for 1 h. After completion of the reaction (monitored by TLC), the mixture was diluted with water (2 mL) and EtOAc (5 mL). The supernatant EtOAc solution was decanted. The aqueous layer/portion was extracted with EtOAc (2 × 5 mL). The combined EtOAc extracts were dried (Na_2SO_4) and concentrated under vacuum. The crude reaction mixture was recrystallized from EtOH to obtain the pure pale yellow solid product.

Computational Methods. The ground-state and transition-state structures were optimized using the hybrid meta exchange correlation functional M06-2X with 6-31+G(d) basis set.[29] Truhlar's M06-2X functional has been successful for the calculation of accurate thermochemistry, reaction barriers, and noncovalent interactions present in the reactions involving main group elements.[30] Vibrational frequencies were calculated to ensure that the located minima and transition states were characterized by zero and one imaginary frequencies respectively and to obtain the zero point energy (ZPE) corrections to the energies. Relaxed intrinsic reaction coordinate scans were performed to confirm that the located saddle points do connect the reactants and products (or intermediates).[31] Basis set super position errors (BSSE) were calculated using a counterpoise correction scheme, whenever necessary.[32] All structural calculations were done using standard quantum chemistry programs.[33]

Experimental Details on Spectroscopy. The steady-state absorption and emission spectra were recorded in a UV spectrophotometer (Cary100, Varian) and FluoroMax-3 spectrofluorimeter, respectively. All experiments were carried out at room temperature (298 K). We have taken 25 μM concentration of catalyst **1** or **2** in each measurement.

■ ASSOCIATED CONTENT

Supporting Information

The following files are available free of charge on the ACS Publications website at DOI: 10.1021/cs5010695.

Experimental procedure, spectroscopic data, and scanned spectra; Cartesian coordinates, vibrational frequencies, and energies for all of the optimized geometries; and additional results from the spectroscopy and calculations (PDF).

■ AUTHOR INFORMATION

Corresponding Authors

*E-mail: swadhin.mandal@iiserkol.ac.in.
*E-mail: spad@iacs.res.in.
*E-mail: prasunchem@iiserkol.ac.in.

Notes

The authors declare no competing financial interest.

■ ACKNOWLEDGMENTS

S.K.M. thanks SERB grant No. SR/S1/IC-25/2012 (DST), New Delhi for financial support. S.R.R. and A.P. thank CSIR and SERB (DST) for RA fellowships, respectively. P.K.V. thanks UGC for a research fellowship. A.D. is grateful to the DST and INSA for partial support. The authors also acknowledge the NMR facility of IISER-Kolkata.

■ REFERENCES

(1) Reid, D. H. *Quart. Rev.* **1965**, *19*, 274−302.
(2) Reid, D. H. *Tetrahedron* **1958**, *3*, 339−352.
(3) (a) Haddon, R. C. *Nature* **1975**, *256*, 394−396. (b) Haddon, R. C. *Aust. J. Chem.* **1975**, *28*, 2343−2351.
(4) (a) Itkis, M. E.; Chi, X.; Cordes, A. W.; Haddon, R. C. *Science* **2002**, *296*, 1443−1445. (b) Pal, S. K.; Itkis, M. E.; Tham, F. S.; Reed, R. W.; Oakley, R. T.; Haddon, R. C. *Science* **2005**, *309*, 281−284. (c) Mandal, S. K.; Itkis, M. E.; Chi, X.; Samanta, S.; Lidsky, D.; Reed, R. W.; Oakley, R. T.; Tham, F. S.; Haddon, R. C. *J. Am. Chem. Soc.* **2005**, *127*, 8185−8196. (d) Mandal, S. K.; Samanta, S.; Itkis, M. E.; Jensen, D. W.; Reed, R. W.; Oakley, R. T.; Tham, F. S.; Donnadieu, B.; Haddon, R. C. *J. Am. Chem. Soc.* **2006**, *128*, 1982−1994. (e) Bag, P.; Pal, S. K.; Itkis, M. E.; Sarkar, S.; Tham, F. S.; Donnadieu, B.; Haddon, R. C. *J. Am. Chem. Soc.* **2013**, *135*, 12936−12939.
(5) Miller, J. S. *Angew. Chem., Int. Ed.* **2003**, *115*, 27−29.
(6) (a) Morita, Y.; Suzuki, S.; Sato, K.; Takui, T. *Nat. Chem.* **2011**, *3*, 197−204. (b) Hicks, R. G. *Nat. Chem.* **2011**, *3*, 189−191.
(7) (a) Mukherjee, A.; Sen, T. K.; Ghorai, P. K.; Mandal, S. K. *Organometallics* **2013**, *32*, 7213−7224. (b) Sen, T. K.; Mukherjee, A.; Modak, A.; Mandal, S. K.; Koley, D. *Dalton Trans.* **2013**, *42*, 1893−1904. (c) Mukherjee, A.; Sen, T. K.; Ghorai, P. K.; Mandal, S. K. *Sci. Rep.* **2013**, *3*, 2821. (d) Mukherjee, A.; Sen, T. K.; Ghorai, P. K.; Samuel, P. P.; Schulzke, C.; Mandal, S. K. *Chem.—Eur. J.* **2012**, *18*, 10530−10545. (e) Sen, T. K.; Mukherjee, A.; Modak, A.; Ghorai, P. K.; Kratzert, D.; Granitzka, M.; Stalke, D.; Mandal, S. K. *Chem.—Eur. J.* **2012**, *18*, 54−58.
(8) Raman, K. V.; Kamerbeek, A. M.; Mukherjee, A.; Atodiresei, N.; Sen, T. K.; Lazic, P.; Caciuc, V.; Michel, R.; Stalke, D.; Mandal, S. K.; Blugel, S.; Munzenberg, M.; Moodera, J. S. *Nature* **2013**, *493*, 509−513.
(9) (a) Ishihara, K. *Lewis acids in organic synthesis*; Yamamoto, H., Ed.; Wiley-VCH: Weinheim, Germany, 2000; Vol *1*, p 135. (b) Carey, F. A.; Sundberg, R. J. *Advanced Organic Chemistry: Part A: Structure and Mechanisms*, 5th ed.; Springer: Berlin, 2007.
(10) Sereda, O. Tabassum, S.Wilhelm, R. *Lewis Acid Organocatalysts, in Asymmetric Organocatalysis, Topic In Current Organic Chemistry*; List, B., Ed.; Springer: Berlin, 2009; pp 86−117.
(11) Bah, J.; Franzen, J. *Chem.—Eur. J.* **2014**, *20*, 1066−1072.
(12) (a) Franz, K. D.; Martin, R. L. *Tetrahedron* **1978**, *34*, 2147−2152. (b) Haddon, R. C.; Rayford, R.; Hirani, A. M. *J. Org. Chem.* **1981**, *46*, 4587−4588.
(13) (a) Corey, E. J.; Zhang, F. *Angew. Chem., Int. Ed.* **1999**, *38*, 1931−1934. (b) O'Brien, P. *Angew. Chem., Int. Ed.* **1999**, *38*, 326−329. (c) Johannes, C. W.; Visser, M. S.; Weatherhead, G. S.; Hoveyda, A. H. *J. Am. Chem. Soc.* **1998**, *120*, 8340−8347. (d) Ager, D. J.; Prakash, I.; Schaad, D. R. *Chem. Rev.* **1996**, *96*, 835−876. (e) Li, G.; Chang, H. T.; Sharpless, K. B. *Angew. Chem., Int. Ed.* **1996**, *35*, 451−454.
(14) (a) Posner, G. H.; Rogers, D. Z. *J. Am. Chem. Soc.* **1977**, *99*, 8208−8214. (b) Carre, M. C.; Houmounou, J. P.; Caubere, P. *Tetrahedron Lett.* **1985**, *26*, 3107−3110. (c) Cossy, J.; Bellosta, V.;

Hamoir, C.; Desmurs, J. R. *Tetrahedron Lett.* **2002**, *43*, 7083−7086. (d) Papini, A.; Ricci, I.; Taddei, M.; Seconi, G.; Dembach, P. *J. Chem. Soc., Perkin Trans.* **1984**, 2261−2265. (e) Fujiwara, M.; Imada, M.; Baba, A.; Matsuda, H. *Tetrahedron Lett.* **1989**, *30*, 739−740. (f) Fan, R. H.; Hou, X. L. *J. Org. Chem.* **2003**, *68*, 726−730. (g) Chakraborti, A. K.; Rudrawar, S.; Kondaskar, A. *Org. Biomol. Chem.* **2004**, *2*, 1277−1280. (h) Bonollo, S.; Fringuelli, F.; Pizzo, F.; Vaccaro, L. *Synlett* **2008**, *10*, 1574−1578 DOI: 10.1055/s-2008-1078410.

(15) (a) Yamada, J. I.; Yumoto, M.; Yamamoto, Y. *Tetrahedron Lett.* **1989**, *30*, 4255−4258. (b) Yamamoto, Y.; Asao, N.; Meguro, M.; Tsukade, N.; Nemoto, H.; Adayari, N.; Wilson, J. G.; Nakamura, H. *J. Chem. Soc. Chem. Commun.* **1993**, 1201−1203. (c) Chini, M.; Crotti, P.; Favero, L.; Machhia, F.; Pineschi, M. *Tetrahedron Lett.* **1994**, *35*, 433−436. (d) Meguro, M.; Asao, N.; Yamamoto, Y. *J. Chem. Soc., Perkin Trans.* **1994**, *1*, 2597−2601. (e) Auge, J.; Leroy, F. *Tetrahedron Lett.* **1996**, *37*, 7715−7716. (f) Sekar, G.; Singh, V. K. *J. Org. Chem.* **1999**, *64*, 287−289. (g) Sagava, S.; Abe, H.; Hase, Y.; Inaba, T. *J. Org. Chem.* **1999**, *64*, 4962−4965. (h) Pujala, B.; Rana, S.; Chakraborti, A. K. *J. Org. Chem.* **2011**, *76*, 8768−8780.

(16) (a) Bonnet-Delpon, D.; Begue, J.-P. *J. Org. Chem.* **2000**, *65*, 6749−6751. (b) Yadav, J. S.; Reddy, B. V. S.; Basak, A. K.; Narsaiah, A. V. *Tetrahedron Lett.* **2003**, *44*, 1047−1050. (c) Surendra, K.; Krishnaveni, N. S.; Rao, K. R. *Synlett* **2005**, 506−510 DOI: 10.1055/s-2005-862359. (d) Azizi, N.; Saidi, M. R. *Org. Lett.* **2005**, *7*, 3649−3651.

(17) Sarkar, A.; Tham, F. S.; Haddon, R. C. *J. Mater. Chem.* **2011**, *21*, 1574−1581.

(18) Chi, X.; Itkis, M. E.; Patrick, B. O.; Barclay, T. M.; Reed, R. W.; Oakley, R. T.; Cordes, A. W.; Haddon, R. C. *J. Am. Chem. Soc.* **1999**, *121*, 10395−10402.

(19) (a) Lakowicz, J. R. *Principles of Fluorescence Spectroscopy*, 3rd ed.; Plenum Press: New York, 1999. (b) Egli, M.; Sarkhel, S. *Acc. Chem. Res.* **2007**, *40*, 197−205. (c) Mooibroek, T. J.; Gamez, P.; Reedijk, J. *CrystEngComm.* **2008**, *10*, 1501−1515.

(20) Sharma, U.; Togati, N.; Maji, A.; Manna, S.; Maiti, D. *Angew. Chem., Int. Ed.* **2013**, *52*, 12669−12673.

(21) For examples of proton transfer mechanisms assisted by counterion or other cooperative mechanisms, see (a) Dudnik, A. S.; Xia, Y.; Li, Y.; Gevorgyan, V. *J. Am. Chem. Soc.* **2010**, *132*, 7645−7655. (b) Xia, Y.; Dudnik, A. S.; Gevorgyan, V.; Li, Y. *J. Am. Chem. Soc.* **2008**, *130*, 6940−6941. (c) Shao, Z.; Zhang, H. *Chem. Soc. Rev.* **2009**, *38*, 2745−2755. (d) Masuda, Y.; Mori, Y.; Sakurai, K. *J. Phys. Chem. A* **2013**, *117*, 10576−10587. (e) Nijamudheen, A.; Jose, D.; Datta, A. *J. Phys. Chem. C* **2011**, *115*, 2187−2195. (f) Patil, N. T.; Nijamudheen, A.; Datta, A. *J. Org. Chem.* **2012**, *77*, 6179−6185.

(22) The calculations predict that the formation of **7** and **8** (in Figure 7) are endothermic processes and the reverse reactions to go back to the weakly bound noncovalent adduct **6** should be very fast ($\Delta G^{\ddagger}$ = 0.5 and 4.8 kcal/mol only). Therefore, in a mixture of **1** and **4a**, the much smaller populations of the structures **7** and **8** compared to **6** makes the detection of **7** and **8** by spectroscopy intractable.

(23) (a) Chakraborti, A. K.; Raha Roy, S.; Kumar, D.; Chopra, P. *Green Chem.* **2008**, *10*, 1111−1118. (b) Wang, S. Y.; Ji, S.-J. *Synth. Commun.* **2008**, *38*, 1291−1298. (c) Kamble, V. T.; Kadama, K. R.; Joshia, N. S.; Muleya, D. B. *Catal. Commun.* **2007**, *8*, 498−502. (d) Firouzabadi, H.; Iranpoor, N.; Jafari, A. A. *J. Mol. Catal. A: Chem.* **2006**, *244*, 168−172. (e) Deb, M. L.; Bhuyan, P. J. *Tetrahedron Lett.* **2006**, *47*, 1441−1443. (f) Wang, L.-M.; Han, J.-W.; Tian, H.; Sheng, J.; Fan, Z.-Y.; Tang, X.-P. *Synlett* **2005**, *2*, 337−340. (g) Zhang, Z. H.; Yin, L.; Wang, Y.-M. *Synthesis* **2005**, *12*, 1949−1954 DOI: 10.1055/s-2005-869959. (h) Mo, L.-P.; Chuan, Z.; Zhang, Z.-H. *Synth. Commun.* **2005**, *35*, 1997−2004. (i) Singh, P. R.; Singh, D. U.; Samant, S. D. *Synth. Commun.* **2005**, *35*, 2133−2138. (j) Ji, S.-J.; Wang, S.-Y.; Zhang, Y.; Loh, T.-P. *Tetrahedron* **2004**, *60*, 2051−2055.

(24) (a) Casapullo, A.; Bifulco, G.; Bruno, I.; Riccio, R. *J. Nat. Prod.* **2000**, *63*, 447−451. (b) Garbe, T. R.; Kobayashi, M.; Shimizu, N.; Takesue, N.; Ozawa, M.; Yukawa, H. *J. Nat. Prod.* **2000**, *63*, 596−598. (c) Bao, B.; Sun, Q.; Yao, X.; Hong, J.; Lee, C. O.; Sim, C. J.; Im, K. S.; Jung, J. H. *J. Nat. Prod.* **2005**, *68*, 711−715.

(25) Sundberg, R. J. *The Chemistry of Indoles*; Academic Press: New York, 1996.

(26) (a) Corey, E. J.; Clark, D. A.; Goto, G.; Marfat, A.; Mioskowski, C.; Sameulson, B.; Hammerson, S. *J. Am. Chem. Soc.* **1980**, *102*, 1436−1439. (b) Luly, J. R.; Yi, N.; Soderquist, J.; Stein, H.; Cohen, J.; Perun, T. J.; Plattner, J. J. *J. Med. Chem.* **1987**, *30*, 1609−1616. (c) Hashiyama, T. *Med. Res. Rev.* **2000**, *20*, 485−501. For review: (d) Domling, A. *Chem. Rev.* **2006**, *106*, 17−89. (e) Zhu, J.*Multicomponent Reactions*; Bienayme, H., Ed.; Wiley-VCH: Weinheim, Germany, 2005. (f) Wipf, P.; Stephenson, C. R. J.; Okumura, K. *J. Am. Chem. Soc.* **2003**, *125*, 14694−14695.

(27) (a) Das, B.; Laxminarayana, K.; Ravikanth, B.; Rao, B. R. *J. Mol. Catal. A: Chem.* **2007**, *261*, 180−183. (b) Nagarapu, L.; Baseeruddin, M.; Apuri, S.; Kantevari, S. *Catal. Commun.* **2007**, *8*, 1729−1734. (c) Khodaei, M. M.; Khosropour, A. R.; Moghanian, H. *Synlett* **2006**, *6*, 916−920. (d) Patil, S. B.; Singh, P. R.; Surpur, M. P.; Samant, S. D. *Ultrason. Sonochem.* **2007**, *14*, 515−518. (e) Lei, M.; Ma, L.; Hu, L. *Tetrahedron Lett.* **2009**, *50*, 6393−6397.

(28) (a) Juaristi, E. *Enantioselective Synthesis of β-Amino Acids*; Wiley: New York, 1997. (b) Knapp, S. *Chem. Rev.* **1995**, *95*, 1859−1876. (c) Wang, Y.-F.; Izawa, T.; Kobayashi, S.; Ohno, M. *J. Am. Chem. Soc.* **1982**, *104*, 6465−6466. (d) Dingermann, T.; Steinhilber, D.; Folkers, G.*Front Matter in Molecular Biology in Medicinal Chemistry*; Wiley-VCH: Weinheim, Germany, 2004. (e) Shen, A. Y.; Tsai, C. T.; Chen, C. L. *Eur. J. Med. Chem.* **1999**, *34*, 877−882. (f) Shen, A. Y.; Chen, C. L.; Lin, C. I. *Chin. J. Physiol.* **1992**, *35*, 45−52.

(29) (a) Zhao, Y.; Schultz, N. E.; Truhlar, D. G. *J. Chem. Theory Comput.* **2006**, *2*, 364−382. (b) Zhao, Y.; Truhlar, D. G. *Theor. Chem. Acc.* **2008**, *120*, 215−241. (c) Hariharan, P. C.; Pople, J. A. *Theor. Chim. Acta* **1973**, *28*, 213−222.

(30) (a) Jissy, A. K.; Datta, A. *J. Phys. Chem. Lett.* **2013**, *4*, 1018−1022. (b) Nijamudheen, A.; Jose, D.; Shine, A.; Datta, A. *J. Phys. Chem. Lett.* **2012**, *3*, 1493−1496. (c) Pieniazek, S. N.; Clemente, F. R.; Houk, K. N. *Angew. Chem., Int. Ed.* **2008**, *47*, 7746−7749. (d) Wheeler, S. E.; Houk, K. N.; Schleyer, P. V. R.; Allen, W. D. *J. Am. Chem. Soc.* **2009**, *131*, 2547−2560.

(31) (a) Fukui, K. *Acc. Chem. Res.* **1981**, *14*, 363−368. (b) Hratchian, H. P.; Schlegel, H. B. *J. Chem. Phys.* **2004**, *120*, 9918−9924.

(32) Boys, S. F.; Bernardi, F. *Mol. Phys.* **1970**, *19*, 553−566.

(33) Frisch, M. J.; Trucks, G. W.; Schlegel, H. B.; Scuseria, G. E.; Robb, M. A.; Cheeseman, J. R.; Scalmani, G.; Barone, V.; Mennucci, B.; Petersson, G. A.; et al. *Gaussian 09*; Gaussian, Inc.: Wallingford, CT, 2009.